803. An adaptive lifting scheme and its application in rolling bearing fault diagnosis

Hongkai Jiang[1], Chendong Duan[2]
[1] School of Aeronautics, Northwestern Polytechnical University, Xi'an 710072, China
[2] School of Electronic & Control Engineering, Chang'an University, Xi'an 710064, China
E-mail: [1]*jianghk@nwpu.edu.cn*, [2]*cdduan@chd.edu.cn*

(Received 4 March 2012; accepted 14 May 2012)

Abstract. Vibration signals of rolling bearings usually are corrupted by heavy noise and it is very important to extract fault features from such signals. In this paper, an adaptive lifting scheme is proposed for fault diagnosis of rolling bearings. The kurtosis indexes of scale decomposition signals are used as the optimization indicator to select the prediction operator and update operator, which can adapt to the dominant signal characteristics, and reveal the fault feature. Fourier transform is adopted to remove the overlapping signal frequency components at every scale decomposition signal. Experimental results confirm the advantage of the adaptive lifting scheme over lifting scheme for feature extraction, and the typical features of rolling bearing in time domain are successfully extracted by adaptive lifting scheme.

Keywords: adaptive lifting scheme, kurtosis index, rolling bearing, fault diagnosis.

1. Introduction

Rolling bearings are widely used in modern machines, such as aircraft engines, generators, etc. Rolling bearing fault diagnosis via vibration signal is the common method for monitoring the condition of a bearing [1]. However when there exists a rolling bearing fault, especially at the early stage, the defect feature information usually is weak and overwhelmed by heavy noise. The heavy noise contains wide frequency band noise and higher-level macro-structural vibrations, and it is difficult to detect rolling bearing defect feature from such heavy noise vibration signal. An effective signal processing method would be necessary to remove such corrupting noise interference.

Many studies have been carried out for rolling bearing fault diagnosis, such as cepstrum analysis [2], cyclic Wiener filter [3], modified morphological method [4], hidden Markov models [5]. These methods have proved their effectiveness for rolling bearing fault diagnosis.

Wavelet provides multiresolution analysis and signal decompositions in independent frequency bands. It has become a powerful tool for rolling bearing fault diagnosis. Wang et al. [6] adopted multiwavelet denoising method for rolling bearing fault diagnosis. Su et al. [7] utilized optimal Morlet wavelet filter and autocorrelation enhancement to extract rolling bearing fault feature. Cheng et al. [8] used continuous wavelet transform to construct impulse response wavelet to detect faults from rolling bearing vibration signals.

In all the wavelet techniques mentioned above, researchers usually selected a fixed wavelet function from a library of previously designed wavelet functions, and the wavelet function does not dynamically match a specific fault symptom. In addition, there exists the overlap of the decomposition frequency bands, namely, the high frequency signal components occur in the low frequency band and the low frequency signal components occur in the high frequency band [9]. New wavelet method is needed to overcome the drawbacks.

Lifting scheme was put forward by Sweldens [10-12], which is a spatial domain construction of biorthogonal wavelet. Compared with classical wavelet transform, lifting scheme provides a great deal of flexibility, which means that any linear, non-linear, or space-varying prediction operator and update operator can be used, and it ensures that the resulting transform is invertible. Many researchers has used lifting scheme for fault diagnosis [13-15].

In this paper, an adaptive lifting scheme is presented. It is designed to capture the impulse feature of the rolling bearing vibration by adaptive decomposition. Lifting scheme is reviewed in

Section 2. In Section 3, the prediction operator and update operator are adaptive selected according to the kurtosis index. Lifting filter frequency domain overlap is analyzed in Section 4. In Section 5, an adaptive lifting scheme and rolling bearing fault diagnosis procedures are proposed. In Section 6, the adaptive lifting scheme is applied to analyze the experimental rolling bearing vibration signal. Comparison with lifting scheme is shown. Conclusions are given in Section 7.

2. Lifting scheme

Lifting scheme includes three procedures as following [10-12].

Split: Suppose $x(n)$ is the original signal set, it is divided into even subset $x_e(n)$ and odd subset $x_o(n)$, where $n \in Z$:

$$x_e(n) = x(2n) \tag{1}$$

$$x_o(n) = x(2n-1) \tag{2}$$

Predict: The odd subset $x_o(n)$ is predicted by even subset $x_e(n)$ with prediction operator $P = [p_1, ..., p_N]$, where N is the number of prediction coefficient. The prediction difference $d(n)$ is defined as the wavelet detail signal:

$$d(n) = x_o(n) - p_1 x_e(n - D + 1) - ... - p_N x_e(n + D) \tag{3}$$

where $D = N / 2$.

Update: The wavelet approximation signal $c(n)$ is obtained by combining the even subset $x_e(n)$ and the detail signal $d(n)$ with update operator $U = [u_1, ..., u_{\tilde{N}}]$., where $\tilde{N}$ is the update coefficient. $c(n)$ is defined as follows:

$$c(n) = x_e(n) + u_1 d(n - \tilde{D}) + ... + u_{\tilde{N}} d(n + \tilde{D} - 1) \tag{4}$$

where $\tilde{D} = \tilde{N} / 2$.

P and U are calculated by the following steps.

Construct a $N \times N$ matrix E, its elements are as following:

$$\left[E\right]_{i,j} = \left[2j - N - 1\right]^{i-1} \tag{5}$$

where $i = 1, 2, ..., N$; $j = 1, 2, ..., N$. P is calculated with the following equation:

$$EP = \left[1, 0, 0, ..., 0\right]^T \tag{6}$$

Given a matrix $Q = [q_1, ..., q_{2N+2\tilde{N}-3}]$, its elements are as follows:

$$q_{2l-1} = \begin{cases} 1 - \sum_{i=1}^{N} p_i u_{l-i+1}, & l = (N + \tilde{N}) / 2 \\ \sum_{i=1}^{N} p_i u_{l-i+1}, & l \neq (N + \tilde{N}) / 2 \end{cases} \tag{7}$$

$$q_{2+N-2} = u_l, \quad l = 1, 2, ..., \tilde{N} \tag{8}$$

$$q_{2l} = 0, \quad l = \text{others} \tag{9}$$

Construct a $\tilde{N} \times (2N + 2\tilde{N} - 3)$ matrix $\tilde{E}$, its elements are:

$$\left[\tilde{E}\right]_{m,n} = n^m \tag{10}$$

where $n = -N - \tilde{N} + 2, -N - \tilde{N} + 3, ..., N + \tilde{N} - 2, m = 0, 1, ..., \tilde{N} - 1$.

U is calculated with the following equation:

$$\tilde{E}Q = 0 \tag{11}$$

Lifting scheme wavelet functions and scaling functions are calculated from P and U by iteration algorithm [16]. The different number combinations of prediction operator coefficients and update operator coefficients $(N, \tilde{N})$ can generate different characteristics of lifting scheme wavelet functions and scaling functions (Fig. 1).

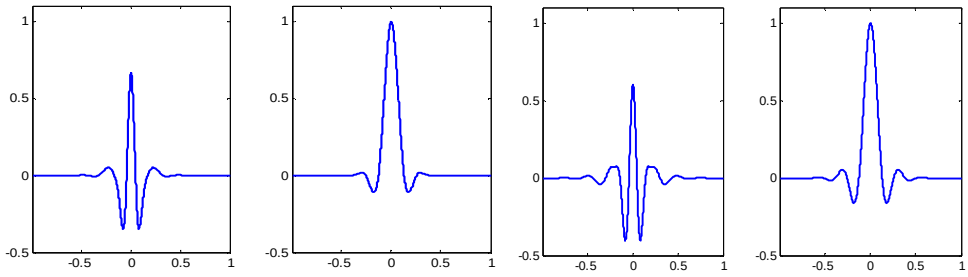

Fig. 1. Lifting scheme wavelet function and scaling function characteristics: (a) (6, 4) and (b) (14, 12)

3. Adaptive selection of lifting scheme operators

Lifting scheme increases the flexibility for adaptive wavelet transform construction. From Equations (3) and (4), we can choose the coefficient number N and $\tilde{N}$ of prediction operator coefficients and update operator according to signal characteristics.

Kurtosis index is sensitive to abrupt vibration signals such as impulses caused by rolling bearing surface defect fault. At the early stage, the more serious the fault is, the larger the kurtosis index is [2, 17, 18]. The kurtosis index of vibration signal is calculated using the following equation:

$$kur = \frac{\frac{1}{M}\sum_{n=1}^{M}(x(n) - \overline{x})^4}{\left[\frac{1}{M}(x(n) - \overline{x})^2\right]^2} \tag{12}$$

where *kur* denotes signal kurtosis value, $x(n)$ is the sample value, M is the sample number, and $\bar{x}$ is the sample mean value. Since kurtosis index can reflect rolling bearing defect fault severity degree, in this paper, we use kurtosis index of scale decomposition signal as the optimization indicator to select the appropriate prediction operator and update operator, which can adaptively lock on to the rolling bearing fault features.

3. 1 Prediction operator selection

Select different coefficient number N_1, N_2, and N_3 of prediction operator and calculate the scale detail signals using Equation (3). In this paper N_1, N_2 and N_3 are 4, 6, 8, namely the prediction operator coefficients are [-0.0625, 0.5625, 0.5625, -0.0625], [0.0117, -0.0977, 0.5859, 0.5859, -0.0977, 0.0117] and [-0.0024, 0.0239, -0.1196, 0.5981, 0.5981, -0.1196, 0.0239, -0.0024], respectively. These prediction operators are usually selected for mechanical fault diagnosis, which can effectively extract fault features [19].

From N_1, N_2 and N_3, select the prediction operator Padapt which has the maximum kurtosis index of scale detail signal as the prediction operator at the decomposition scale, and its prediction result is used as the detail signal.

3. 2 Update operator selection

Select different coefficient number $\tilde{N}_1$, $\tilde{N}_2$ and $\tilde{N}_3$ of update operator and calculate the scale approximation signals using Equation (4). In this paper $\tilde{N}_1$, $\tilde{N}_2$ and $\tilde{N}_3$ are 4, 6, 8, namely the update operator coefficients are [-0.0313, 0.2813, 0.2813, -0.0313], [0.0059, -0.0488, 0.2930, 0.2930, -0.0488, 0.0059] and [-0.0012, 0.0120, -0.0598, 0.2991, 0.2991, -0.0598, 0.0120, -0.0012], respectively. These update operators are usually selected for mechanical fault diagnosis, which can effectively extract fault features [19].

The kurtosis of each approximation signal is calculated using Equation (12). From $\tilde{N}_1$, $\tilde{N}_2$ and $\tilde{N}_3$, select the update operator Uadapt which has the maximum kurtosis index of approximation signal as the update operator at the decomposition scale, and its update result is used as the approximation signal.

4. Lifting filter

Lifting scheme can be presented in polyphase matrix form [20]. Polyphase matrix constructs the connection between the lifting operators and lifting filter, from which we can obtain the frequency characteristics of lifting filter.

4. 1 Lifting filter calculation

Claypool gave the polyphase matrix *z*-transform from prediction and update step, and the lifting filter is defined as follows [20]:

$$\left.\begin{aligned}\tilde{g}(z) &= -P(z^2) + z^{-1} \\ \tilde{h}(z) &= 1 - P(z^2)U(z^2) + z^{-1}U(z^2)\end{aligned}\right\} \quad (13)$$

where $\tilde{g}$ and $\tilde{h}$ are the lifting decomposition high-pass filter and low-pass filter, respectively.

From Equation (13), we can further deduce the coefficients of $\tilde{g}$ from the coefficients of P as follows:

$$\left.\begin{aligned}\tilde{g}(2l-1) &= -p(l) \\ \tilde{g}(2l) &= \delta(l-N/2)\end{aligned}\right\} \tag{14}$$

where $l = 1, 2, ..., N$.

The coefficients of $\tilde{h}$ are deduced from the coefficients of P and U as following:

$$\tilde{h}(2i) = \begin{cases} -\sum_{j=1}^{i} p(j)u(i-j+1), & i < \tilde{N} \\ 1-\sum_{j=1}^{N} p(j)u(i-j+1), & i = (N+\tilde{N})/2 \\ -\sum_{j=1}^{\tilde{N}} u(j)p(i-j+1), & \tilde{N} \le i < (N+\tilde{N})/2 \end{cases} \tag{15}$$

$$\tilde{h}(N+\tilde{N}+2i-2) = \tilde{h}(N+\tilde{N}-2i+2) \tag{16}$$

where $2 \le i \le (N+\tilde{N})/2$.

$$\tilde{h}(2i-1) = u(i-N/2+1) \tag{17}$$

where $N/2 \le i \le (N/2+\tilde{N}-1)$.

$$\tilde{h}(2i-1) = 0 \tag{18}$$

where $(N/2+\tilde{N}-1) < i \le (N+\tilde{N}-2)$, $1 \le i < N/2$ and $\tilde{N} < N$.

Since the prediction operator P and update operator U are selected according to the decomposition signal kurtosis index in Section 3, from Equation (14), (15), (16), (17) and (18), the lifting filters can also adaptively match the signal characteristics.

4. 2 Lifting filter frequency domain characteristics

By selecting different combination of prediction operator coefficient number N and updating operator coefficient number $\tilde{N}$ we can obtain different lifting filter frequency characteristics as illustrated in Fig. 2. From Fig. 2, the lifting filter orthogonalty becomes stronger as N and $\tilde{N}$ increase, but lifting filter frequency band overlapping problem is inevitable.

In this paper, we refer to the papers [9, 15], and adopt Fourier transform to solve the lifting filter overlapping problem.

Suppose the approximation signal and detail signal are c_j and d_j adopting lifting scheme, respectively, where j is the decomposition scale. The signal sampling frequency is f_s , then $f_s / 2^j$ is the cut-off frequency point at decomposition scale j . The frequency components in

c_j, which are larger than $f_s / 2^{j+1}$, are set to zeros; while the frequency components in d_j, which are less than $f_s / 2^{j+1}$, are set to zeros. With this procedure, the overlapping signal components at corresponding decomposition scale are removed.

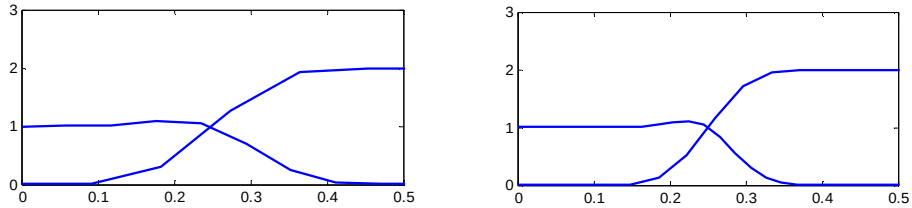

Fig. 2. Lifting filter frequency characteristics: (a) (6, 4) and (b) (14, 12)

5. Adaptive lifting scheme

In this paper, we combine the lifting operator adaptive selection in Section 3 and lifting filter frequency characteristics in Section 4, and propose an adaptive lifting scheme, which is shown in Fig. 3. Padapt denotes adaptive selection prediction operator, Uadapt denotes adaptive selection update operator, rc denotes removing overlapping signal frequency components from approximation signal at scale j, rd denotes removing overlapping signal frequency components from detail signal at scale j, separately.

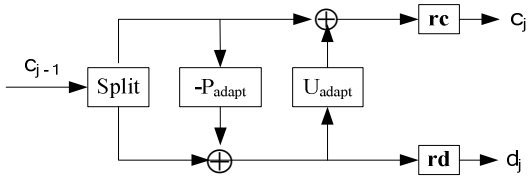

Fig. 3. Adaptive lifting scheme

The procedures of adaptive lifting scheme for rolling bearing fault diagnosis are as follows:

1) Prediction and update operators adaptive selection.

Rolling bearing vibration signal is decomposed using different prediction and update operators at each scale. The prediction and update operators, with which the kurtosis indexes of scale decomposition signals have the maximum values, are selected.

2) Overlapping signal frequency components removing.

The overlapping signal frequency components in detail signal and approximation signal at each scale are removed using Fourier transform.

3) Rolling bearing fault diagnosis.

Rolling bearing fault characteristics are extracted with the results of adaptive lifting scheme to diagnose rolling bearing defects.

The flow chart of rolling bearing fault diagnosis using the proposed adaptive lifting scheme is shown in Fig. 4.

6. Applications

In this section, we use the proposed adaptive lifting scheme to analyze the experimental signal and engineering signal, followed by extraction of the rolling bearing fault feature.

A rolling bearing experimental test rig is presented in Fig. 5. A rolling bearing with outer raceway defect was mounted on the experimental setup. It is used to verify the validation of the proposed method.

The rolling bearing parameters are listed in Table 1.

Table 1. Rolling bearing parameters

Pitch diameter	225mm
Rolling element diameter	34mm
Rolling element number	17
Contact angle	0^0

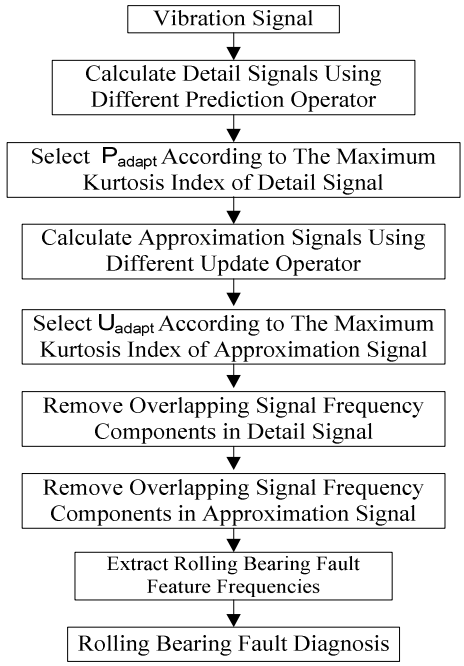

Fig. 4. Flow chart of rolling bearing fault diagnosis

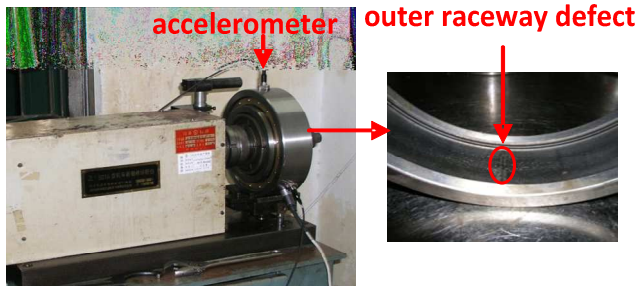

Fig. 5. Rolling bearing test rig

Rotating speed of the test rig shaft was 467 r/min. According to the rolling bearing parameters and rotating speed, the outer race fault characteristic frequency can be calculated using the following equation, and which is equal to 56.2 Hz:

$$f_o = \frac{f}{2}\left(1 - \frac{d}{E}\cos\alpha\right)z \tag{19}$$

where f_o is the outer raceway characteristic fault frequency, f is the shaft rotating frequency, E is the pitch diameter, d is the rolling element diameter, z is the number of rolling elements, and α is the rolling element contact angle.

The rolling bearing vibration signal is provided in Fig. 6. The fault feature is buried in the heavy background noise, there is no useful information. The spectrum of the rolling bearing vibration signal is shown in Fig. 7. The spectrum is complex.

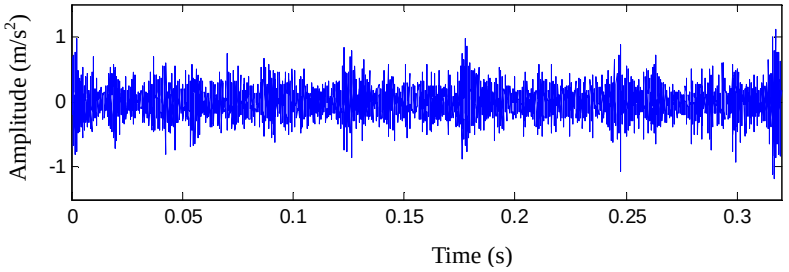

Fig. 6. Rolling bearing vibration signal

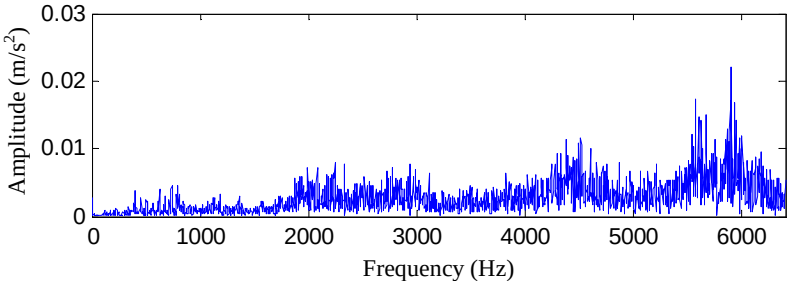

Fig. 7. Rolling bearing vibration signal spectrum

The vibration signal is decomposed into two scales using lifting scheme, and the results are shown in Fig. 8, where d1 is the first scale detail signal, d2 is the second scale detail signal, and c2 is the second scale approximation signal. The decomposition signals are complex, and there are no obvious fault features.

The spectrums of the decomposition signals using lifting scheme are presented in Fig. 9. There exist frequency components overlapping in the decomposition signals.

Using the proposed method in this paper, the vibration signal is decomposed into two scales, and the result is presented in Fig. 10. Evenly spaced impulses can be obviously observed from the approximation signal c2, and the intervals of the impulse are equal to 17.8 ms, which exactly is in accordance with the outer race characteristic fault frequency 56.2 Hz. The outer race fault feature of rolling bearing is extracted successfully.

The spectrums of the decomposition signals using the proposed method are illustrated in Fig. 11. The overlapping signal frequency components are removed in every decomposition signal.

The envelope spectrum of c2 using the proposed method is illustrated in Fig. 12. It mainly consists of the frequency 56.2 Hz and its high-order harmonics, which coincide with the rolling bearing outer race fault characteristic frequency.

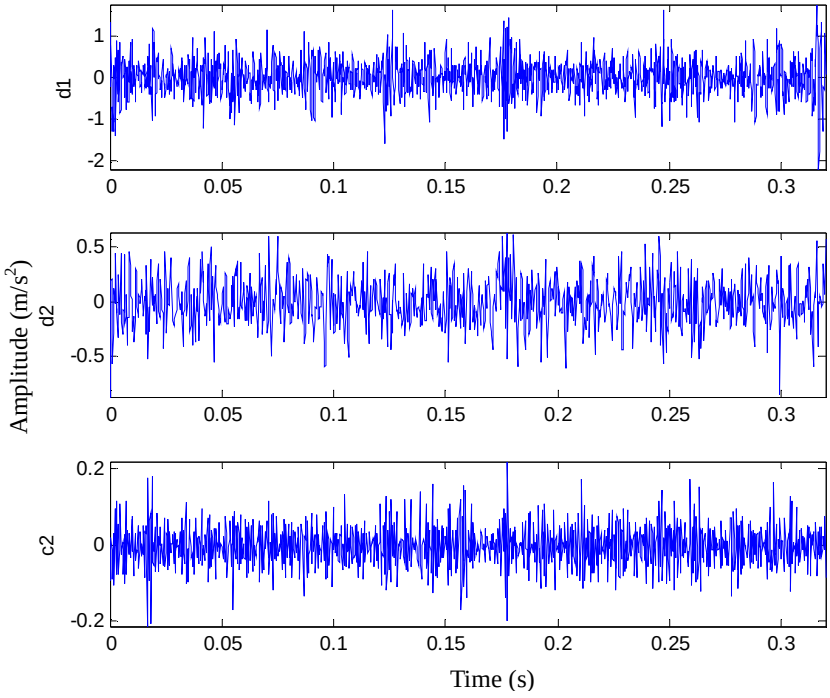

Fig. 8. Lifting scheme decomposition result

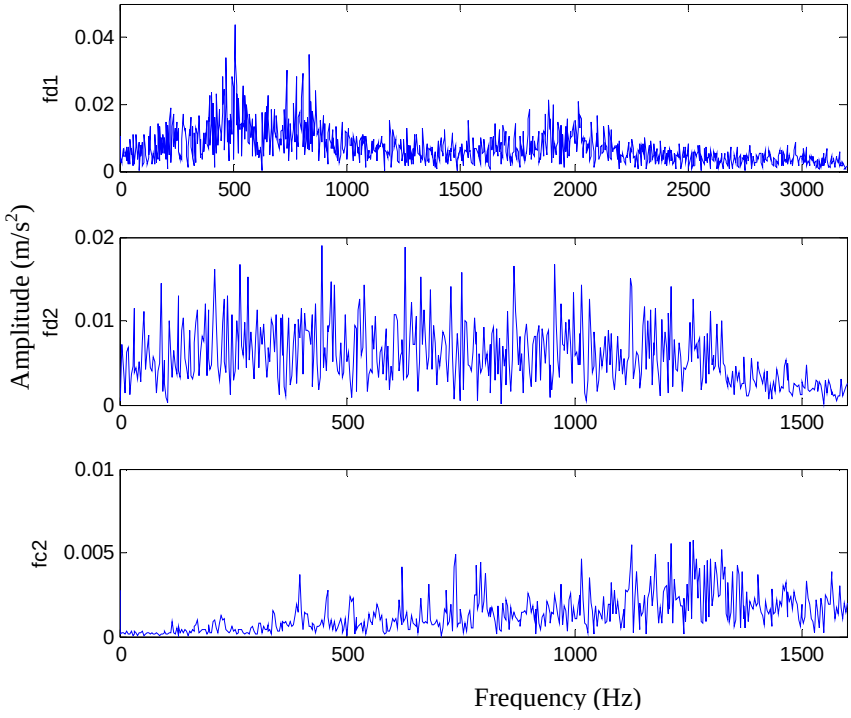

Fig. 9. Lifting scheme decomposition spectrum

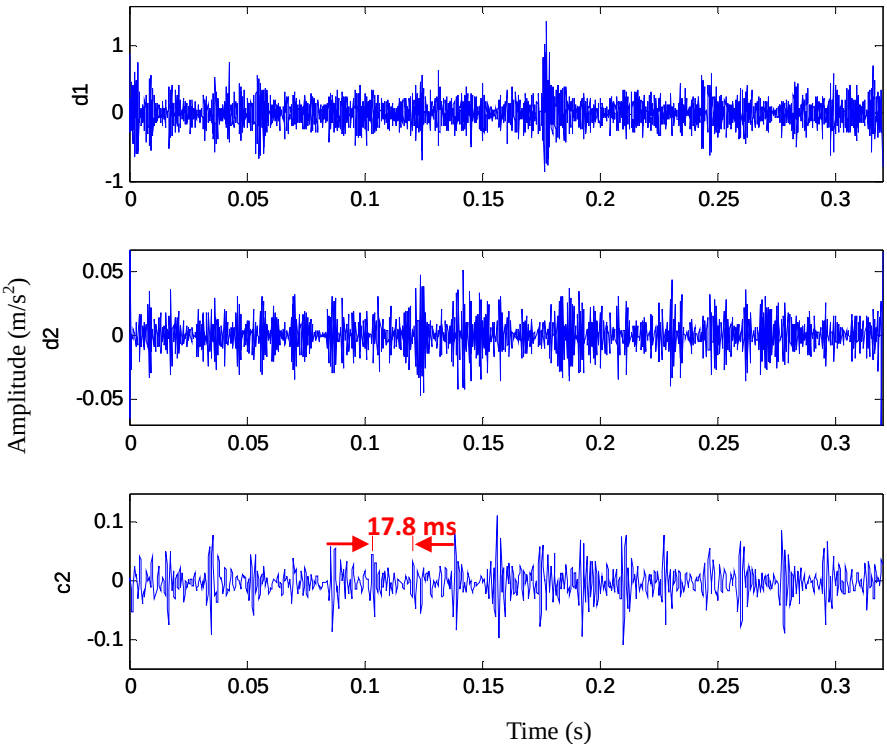

Fig. 10. Proposed method decomposition result

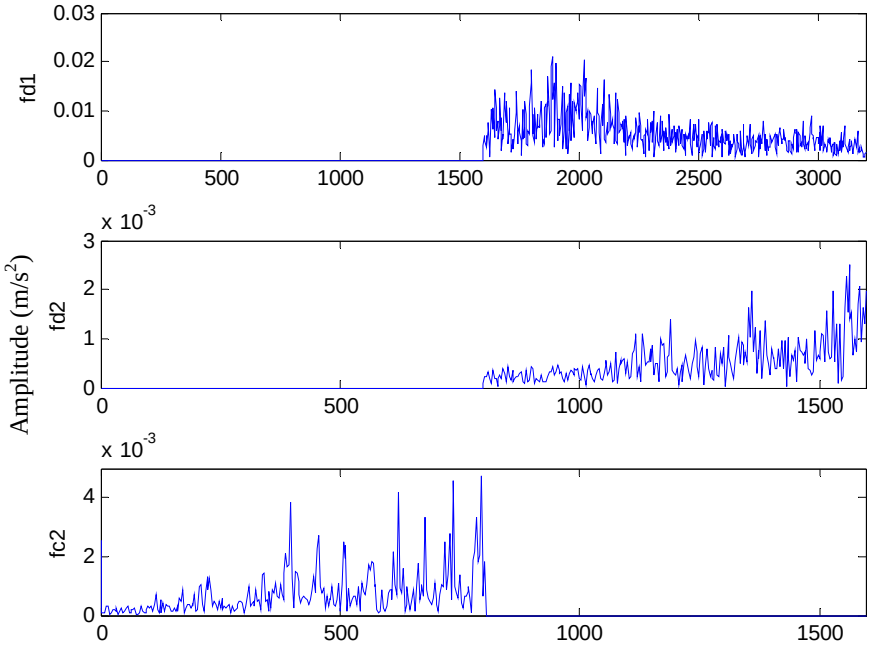

Fig. 11. Proposed method decomposition spectrum

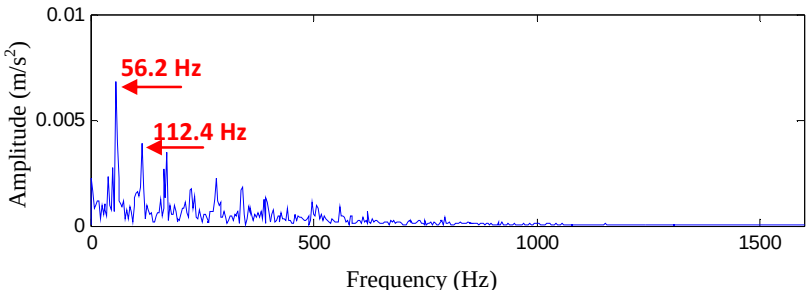

Fig. 12. Proposed method demodulation result of c2

7. Conclusions

Aiming at rolling bearing fault diagnosis under heavy noise background, an adaptive lifting scheme is proposed in this paper. Firstly, the kurtosis indexes of every scale decomposition signals are calculated using different prediction operator and update operator. The prediction operator and update operator, with which the kurtosis indexes have the maximum values and adaptively lock on the fault feature at every decomposition scale, are selected. Then, the overlapping signal frequency components are removed using Fourier transform. The proposed method is validated with the analysis of the experimental signal rolling bearing. The results demonstrate that it performs better than lifting scheme and is very effective in revealing fault features hidden in the vibration signals.

Acknowledgments

This work was supported by the National Natural Science Foundation of China under Grant 50975231.

References

[1] **Immovilli F., Cocconcelli M., Bellini A., Rubini R.** Detection of generalized-roughness bearing fault by spectral-kurtosis energy of vibration or current signals. IEEE Transactions on Industrial Electronics, Vol. 56, 2009, p. 4710-4717.

[2] **Qu L., He Z.** Mechanical Diagnosis. Shanghai Science and Technology Press, China, 1986.

[3] **Ming Y., Chen J., Dong G. M.** Weak fault feature extraction of rolling bearing based on cyclic Wiener filter and envelope spectrum. Mechanical Systems and Signal Processing, Vol. 25, 2011, p. 1773-1785.

[4] **Dong Y. B., Liao M. F., Zhang X. L., Wang F. Z.** Faults diagnosis of rolling element bearings based on modified morphological method. Mechanical Systems and Signal Processing, Vol. 25, 2011, p. 1276-1286.

[5] **Boutros T., Liang M.** Detection and diagnosis of bearing and cutting tool faults using hidden Markov models. Mechanical Systems and Signal Processing, Vol. 25, 2011, p. 2102-2124.

[6] **Wang X. D., Zi Y. Y., He Z. Z.** Multiwavelet denoising with improved neighboring coefficients for application on rolling bearing fault diagnosis. Mechanical Systems and Signal Processing, Vol. 25, 2011, p. 285-304.

[7] **Su W., Wang F., Zhu H., Zhang Z., Guo Z.** Rolling element bearing faults diagnosis based on optimal Morlet wavelet filter and autocorrelation enhancement. Mechanical Systems and Signal Processing, Vol. 24, 2010, p. 1458-2472.

[8] **Cheng J. S., Yu D. J., Yang Y.** Application of an impulse response wavelet to fault diagnosis of rolling bearings. Mechanical Systems and Signal Processing, Vol. 21, 2007, p. 920-929.

[9] **Yang J. G., Park S. T.** An anti-aliasing algorithm for discrete wavelet transform. Mechanical Systems and Signal Processing, Vol. 17, Issue 5, 2003, p. 945-954.

[10] Sweldens W. The lifting scheme: a custom-design construction of biorthogonal wavelets. App. Comput. Harmonic Analysis, Vol. 3, Issue 2, 1996, p. 186-200.
[11] Sweldens W. The lifting scheme: A construction of second generation wavelets. SIAM J. Math. Anal., Vol. 29, Issue 2, 1997, p. 511-546.
[12] Daubechies I., Sweldens W. Factoring wavelet transform into lifting steps. J. Fourier Anal. Appl., Vol. 4, Issue 3, 1998, p. 247-269.
[13] Chen H. X., Chua P. S. K., Lim G. H. Vibration analysis with lifting scheme and generalized cross validation in fault diagnosis of water hydraulic system. Journal of Sound and Vibration, Vol. 301, 2007, p. 458-480.
[14] Li Z., He Z. J., Zi Y. Y., Wang Y. X. Customized wavelet denoising using intra- and inter-scale dependency for bearing fault detection. Journal of Sound and Vibration, Vol. 313, 2008, p. 342-359.
[15] Bao W., Zhou R., Yang J. G., Yu D. R., Li N. Anti-aliasing lifting scheme for mechanical vibration fault feature extraction. Mechanical Systems and Signal Processing, Vol. 23, 2009, p. 1458-1473.
[16] Jiang H., He Z., Duan C., Chen P. Gearbox fault diagnosis using adaptive redundant lifting scheme. Mechanical Systems and Signal Processing, Vol. 20, 2006, p. 1992-2006.
[17] Consolini G., De Michelis P. Non-Gaussian function of AE-index fluctuations: evidence for time intermittency. Geophys. Res. Lett., Vol. 25, 1998, p. 4087-4090.
[18] Sen A. K., Litak G., Edwards K. D., Finney C. E. A., Daw C. S., Wagner R. M. Characteristics of cyclic heat release variability in the transition from spark ignition to HCCI in a gasoline engine. Applied Energy, Vol. 88, 2011, p. 1649-1655.
[19] Duan C. Research on Fault Diagnosis Techniques Using Second Generation Wavelet Transform. Doctorial Thesis, Xi'an Jiaotong University, Xi'an, China, 2005.
[20] Claypoole R. L. Adaptive Wavelet Transforms via Lifting. Doctoral Thesis, Electrical and Computer Engineering, Rice University, Houston, Texas, USA, 1999.